Earthq Eng & Eng Vib (2019) 18: 735-746 **DOI**: https://doi.org/10.1007/s11803-019-0533-6

Numerical study on the fracturing mechanism of shock wave interactions between two adjacent blast holes in deep rock blasting

Yuan Wei[1,2†], Liu Shangge[3†], Wang Wei[1,2‡], Su Xuebin[4†], Li Zonghong[1,2§], Li Jiaxin[1,2§], Wen Lei[1,2†], Chang Jiangfang[1,2†] and Sun Xiaoyun[1,2‡]

1. *School of Civil Engineering, Shijiazhuang Tiedao University, Shijiazhuang 050043, China*
2. *Hebei Technology and Innovation Center on Safe and Efficient Mining of Metal Mines, Shijiazhuang 050043, China*
3. *CCCC Second Highway Consultants Co., Ltd., Wuhan 430056, China*
4. *China National Uranium Co. Ltd., Beijing 100013, China*

Abstract: With the application of electronic detonators, millisecond blasting is regarded as a significant promising approach to improve the rock fragmentation in deep rock blasting. Thus, it is necessary to investigate the fracturing mechanisms of short-delay blasting. In this work, a rectangle model with two circle boreholes is modeled as a particles assembly based on the discrete element method to simulate the shock wave interactions induced by millisecond blasting. The rectangle model has a size of 12 × 6 m (L × W) and two blast holes have the same diameter of 12 cm. The shock waves are simplified as time-varying forces applied at the particles of walls of the two boreholes. Among a series of numerical tests in this study, the spacing between two adjacent boreholes and delay time of millisecond blasting are considered as two primary variables, and the decoupling charge with a coefficient of 1.5 is taken into account in each case. The results show that stress superposition is not a key factor for improving rock fragmentation (tensile stress interactions rather than compressive stress superposition could affect the generation of cracks), whereas collision actions from isolated particles or particles with weakened constraints play a crucial role in creating the fracture network. The delay time has an influence on causing cracks in rock blasting, however, whether it works heavily depends on the distance between the two holes.

Keywords: rock fragmentation; millisecond blasting; shock wave; decoupling charge; discrete element method

1 Introduction

Deep resources, such as nuclear energy, coal methane and geothermal energy *et al*., are always buried a depth of hundreds or up to a thousand meters deep in the earth with complex geological conditions, including high geostress and low permeability. Obviously, they have posed a competitive challenge for the exploitation of these deep resources (Zhu *et al*., 2016; Wang *et al*., 2016). Thus, artificial fracturing techniques are usually implemented to improve the permeability of reservoir rocks to increase the recovery efficiency of deep resources. Among these techniques, controlled blasting is considered to be a promising tool because it is less affected by geological conditions (Zhu *et al*., 2013; Yan *et al*., 2017). Relevant practical blasting has indicated that delayed initiation may yield smaller rock fragments with less vibration than simultaneous initiation. Thus, many scholars have given attention to research on the influence of delay time on fracturing effects in rock blasting (Yi *et al*., 2016).

From the perspective of stress superposition, some researchers have agreed that appropriate delay time has a potential benefit for higher fragmentation than synchronous ignition. In their opinion, the overlap of two or more stress waves may increase the tensile stress around the collision points, which promotes the initiation and propagation of cracks. For instance, Rossmanith (2002) as well as Rossmanith and Kouzniak (2004) have proposed some hypotheses, including the charge length and the velocity of detonation are infinite and the rock mass is homogeneous, elastic and isotropic, to reveal how a positive influence of stress interactions on the cracks generation could be achieved through controlling the ignition times. Vanbrabant and Espinosa (2006) have adopted full-scale tests to clarify that the average

Correspondence to: Wang Wei, School of Civil Engineering, Shijiazhuang Tiedao University, Shijiazhuang 050043, China
Tel: +86-15833964950
E-mail: wangweiuuu@163.com
†Lecturer; ‡Professor; §MSc. Student

Supported by: National Science Foundation for Young Scientists of China under Grant No. 51709176, National Natural Science Foundation of China under Grant No. 51979170, Key Project of Hebei Natural Science Foundation under Grant No. F2019210243, Hebei Province Science Foundation for Young Scientists under Grant No. E2018210046, Open Project of State Key Laboratory of Advanced Electromagnetic Engineering and Technology under Grant No. AEET 2019KF005.
Received November 26, 2017; **Accepted** April 3, 2018

fragmentation could be improved by nearly 50% if the delays between two blast holes create an overlap of the negative tails of the P-wave particle velocity. Chiappetta (2010) has stated that the shock wave interaction could have a good performance if the optimal delay times were short enough so that the shock wave from a previous hole does not reach the next hole before it initiates.

Nevertheless, many academics do not agree with the above opinions and have proposed opposite viewpoints. For example, Cho and Kaneko (2004) have considered five delay times (0, 100, 500, 1000, 2000 microsecond) in bench blasting simulation. Their results showed that simple stress interaction made no difference to the rock fragmentation, and the fragment size oscillated as the delay time increased. However, the optimal fragmentation with respect to delay time depends strongly on the gas flow through the fractures caused by the stress wave. Sjöberg *et al*. (2012) have studied dual-holes blasting and developed a methodology for calculating fragmentation. The results showed that the effect of varying delay time to increasing fragmentation is extremely limited, and the key influencing factors on fragmentation are the spacing between adjacent holes and the amount of explosive charge. Johansson and Ouchterlony (2013) have made a series of small-scale tests associated with bench blasting to study how the short delays facilitate better fragmentation. The final results indicated that there are no distinct improvements of block size when comparing the delayed detonation with no stress wave interactions. Yi *et al*. (2016) have combined the theoretical analysis method with the numerical simulation method to analyze the stress interactions located between two adjacent holes, as well as their extended line. The results showed that stress superposition is local around the collision point, and it would be impossible to improve rock fragmentation by only relying on controlling the stress wave interaction.

In conclusion, the arguments about the influence of stress wave interaction on the rock fragmentation and fragmentation-related delay timing have not been resolved. In this study, the stress superposition is investigated to determine whether or not it could be beneficial to the generation of a fracture network in deep rock blasting. To achieve this goal, a rectangle model with two circle holes is modeled as a particles assembly based on discrete element method. This model has a size of 12 × 6 m (L × W) and two holes have the same diameter of 12 cm. In this study, spacing and delay time of detonation between these two holes are considered as the two primary variables, and the decoupling charge with a coefficient of 1.5 is taken into account in each case. Finally, by analyzing the histories of stress and unbalance force of the monitoring points, the fracturing mechanism of the shock wave interactions between two adjacent blast holes in deep rock blasting is determined.

2 Methodology

2.1 Numerical model

Particle Flow Code (PFC) is a widely used commercial software to simulate the mechanical response of rock subjected to various dynamic and static loads in geotechnical engineering. The rock is modeled as a collection of rounded granules, and the built-in parallel-bond model (PBM) is ideally suited for depicting the force-transferring characteristics of contact between two particles. As shown in Fig. 1, PBM can carry normal force (F_n), shear force (F_s) and bending moment (M), and its mechanical behavior is thought to be analogous to a beam. Thus, the maximum tensile stress (σ_{tmax}) and shear stress (τ_{max}) can be depicted as follows:

$$\begin{cases} \sigma_{t\max} = \dfrac{F_n}{A} + \dfrac{|M|}{I}\bar{R} \\ \tau_{\max} = \dfrac{F_s}{A} \end{cases} \tag{1}$$

In Eq. (1), A is the area of the bond cross section, R is the bond radius, and I is the inertial moment. Once the maximum tensile stress or shear stress exceed the tensile or shear strength of the bond, it indicates that the bond has broken, i.e., a crack between two particles has come into being. Thus, cracks in PFC can be classified into two types: tensile cracks ($\sigma_{t\max} \geq \bar{\sigma}_t$), and shear

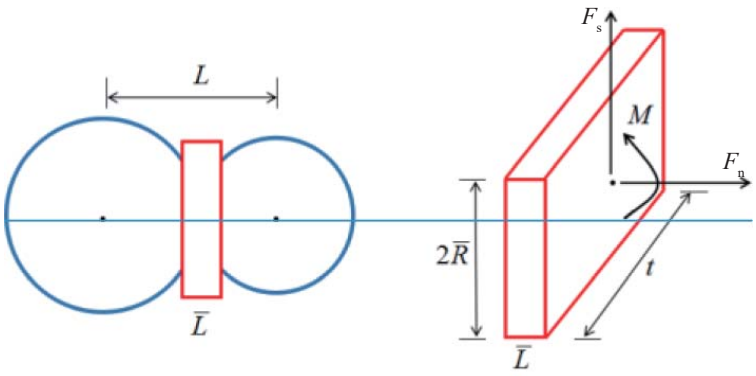

Fig. 1 Form of carrying forces for the PBM in PFC

cracks ($\tau_{max} \geq \overline{\tau}_c$). Here, $\overline{\sigma}_t$ and $\overline{\tau}_c$ represent the tensile and shear strength, respectively (Wang *et al*., 2014; Itasca Consulting Group Inc., 2015).

Figure 2 shows a simplified rock stratum with two blast holes. The model is demonstrated as a rectangle with the size of 12 × 6 m (L × W), and two holes with the same diameter of 12 cm are placed at both sides of the symmetry axis of the rectangle. The distance between two holes is assigned to be three values: 2.0 m, 3.0 m and 4.0 m. The lateral compressive stresses in two directions are both set to be 5.0 MPa, which implies that this model is buried approximately 200 meters in the earth. The model is modeled as a particle assembly composed of 24,762 particles, whose radius conform to uniform distribution and vary from 2 cm to 4 cm.

A key issue for numerical simulation using PFC^{2D} is to establish the relationship between mesoscopic parameters of particles and macroscopic mechanical parameters of rock stratum. Fakhimi and Villegas (2007) have proposed a calibration process to adjust a few main user-changeable mesoscopic parameters of PBM to match desired macroscopic mechanical parameters through numerical simulation experiments, such as a uniaxial compressive test, conventional triaxial compressive test and direct tensile test. Table 1 shows the main mesoscopic parameters of particles, and Fig. 3 shows the loading curves of numerical tests.

According to the Fig. 3(a), the peak value of the "deviatoric stress-axial strain" curve is approximately equal to 86.0 MPa, which manifests the uniaxial compression strength based on the numerical simulation test is 86.0 MPa. In addition, σ_{50} and ε_{l50} located at this "deviatoric stress-axial strain" curve are substituted into Eq. (2) and E of the numerical specimen can be determined to be 46.7 GPa. According to Fig. 3(b), the tensile strength of the numerical specimen can be directly found to be 14.2 MPa. It is generally recognized that three or more triaxial compression tests are required to acquire the c and ϕ of the numerical sample on the basis of the Mohr-Coloumb criterion expressed as Eq. (3). Several different pairs of (σ_3, σ_1) are plotted in the $\sigma_3 - \sigma_1$ coordinate system (seen in Fig. 3(d)). These discrete points are fitted by Eq. (3) to determine its intercept and slope. The c and ϕ of the sample can be easily determined based on the intercept and slope of this linear equation. Five pairs of (σ_3, σ_1) in this study are (0.01, 86.2), (3.0, 98.3), (5.0, 170.7), (7.0, 196.3) and (10.0, 214.1), the computational cohesion and friction angle of this sample are 17.8 MPa and 45.1°, respectively.

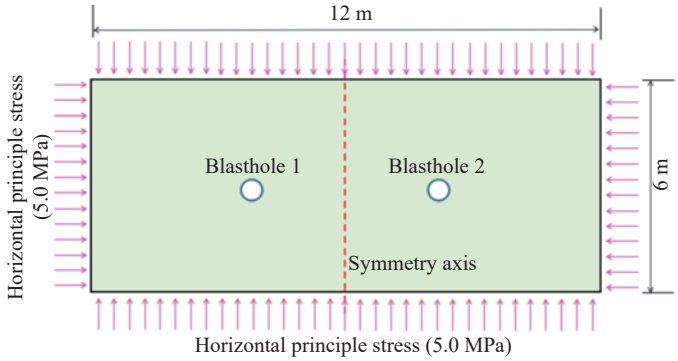

Fig. 2 Simplified model for dual blast holes

Table 1 Main mesoscopic parameters

Linear Group:	Parallel-bond Group:
Grain density = 2750 kg/m^3,	Bond effective modulus = 27.0 GPa,
Effective modulus = 27.0 GPa,	Bond stiffness ratio = 1.0,
Friction coefficient = 0.7,	Bond tensile strength = 32.8 MPa,
Stiffness ratio = 1.0.	Bond cohesion = 150.0 MPa,
	Bond friction angle = 55°.

$$E = \frac{\sigma_{50}}{\varepsilon_{150}} \tag{2}$$

$$\sigma_1 = \frac{1+\sin\phi}{1-\sin\phi}\sigma_3 + \frac{2c\cos\phi}{1-\sin\phi} \tag{3}$$

In Eq. (2), σ_{50} and ε_{150} represent half of the uniaxial compression strength and its corresponding axial strain, respectively.

2.2 Explosive loads

The coefficient of the decoupling charge (ξ) is defined as follow:

$$\xi = \frac{d_b}{d_e} \tag{4}$$

where d_b and d_e are the diameters of the blast hole and cartridge, respectively. Two blast holes' ξ are both set up to be 1.5, and the explosive charges in these holes have the same properties: cartridge diameter $d_e = 8$ cm, explosive density $\rho_e = 1200\ \text{kg/m}^3$, and detonation velocity $D_e = 2700\ \text{m/s}$. According to the elastic wave motion theory, the peak value of the explosive stress wave (p_1) applied at the wall of blast hole can be expressed as (Henrych, 1979; Fakhimi and Villegas, 2007):

$$p_1 = \frac{1}{8}\rho_e D_e^2 \left(\frac{d_e}{d_b}\right)^6 n \tag{5}$$

where n denotes the amplification coefficient of the stress wave, which is generally deemed to be approximately equal to 8.0. To obtain the pressure-time profile of the explosive shock wave, the wave-shape function is needed. In this study, the following expression is adopted to characterize the time evolution curve of explosive stress (Park *et al*., 2004; Dohyun *et al*., 2009):

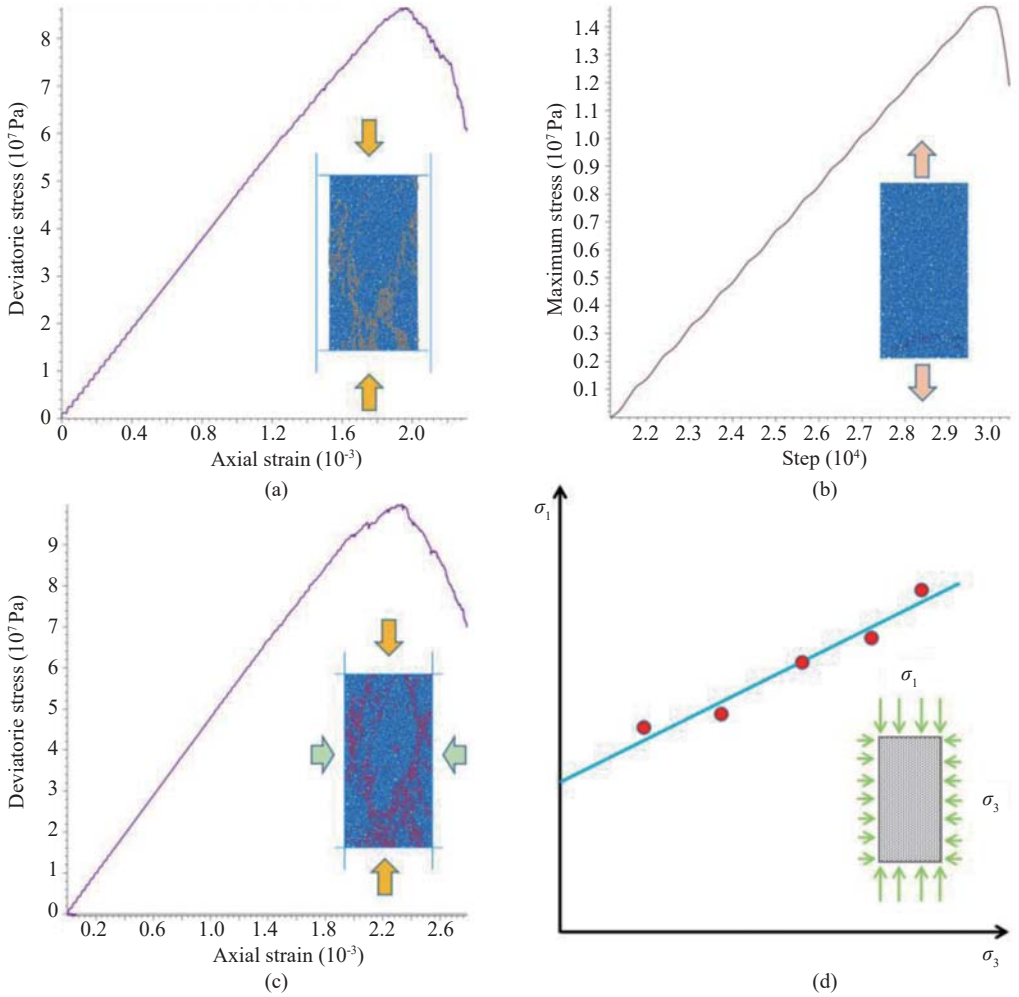

Fig. 3 (a) Simulated PFC^{2D} failure during uniaxial compression test; (b) direct tensile test; (c) tri-axial compression test and (d) fitting of the shear strength

$$f(t)=\frac{t}{t_r}\mathrm{e}^{\left(1-\frac{t}{t_r}\right)} \tag{6}$$

where $f(t)$ is the shape function. t_r is the time to reach peak pressure, which is thought to be 50 μs in this study. Thus, the pressures-time history on the wall of blast holes could be acquired by combining Eq. (5) with Eq. (6), as shown in Fig. 4.

To apply the explosive stress to the wall of the blast hole, the pressure shown in Fig. 4 should be converted into force at each time step. Figure 5 shows a schematic diagram of the force-time history applied on the particles located at the wall of blast hole (shown as green rounded granules). Obviously, the impulse forces exerted at these particles are equal to the transmission pressure, multiplied by their own diameters, and the direction of the shock wave forces are defined from the center of the blast hole towards the center of the particles. Notice that two blast holes are applied to the same explosive stress wave, and the delay times between the two holes are assigned to be 0.0, 0.5, 1.0, 1.5, 2.0, 2.5 ms herein.

3 Results

3.1 Fracture networks

In this study, the focus is on the fracturing effect of the shock wave interaction between two blast holes, so the discussion is concentrated on the distribution

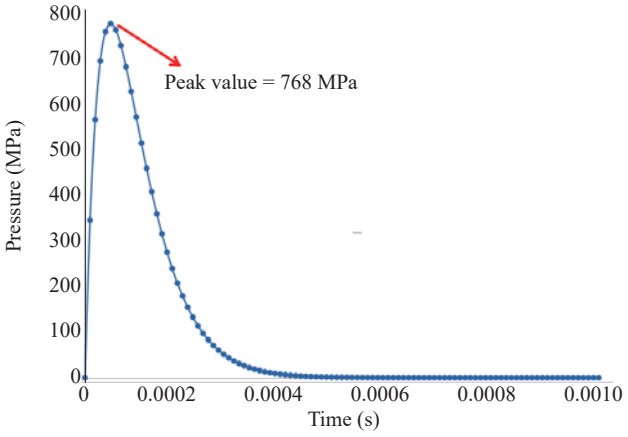

Fig. 4 Pressure-time history in this study (duration time = 1.0 ms)

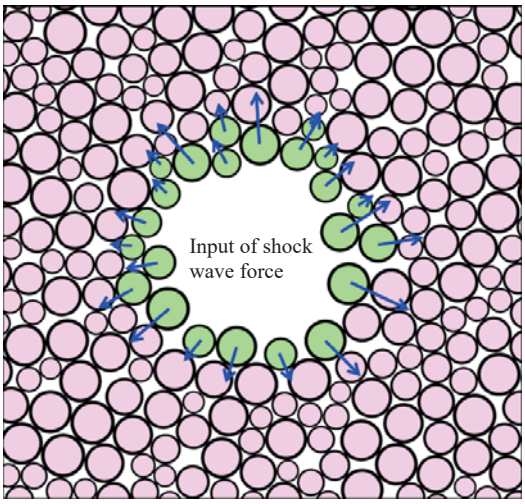

Fig. 5 Schematic diagram of forces applied on the particles of the hole wall

characteristics of the cracks located between these two holes. Figure 6–8 intuitively show the final distributions of cracks induced by blasting at different delay times for the three spacings of the two blast holes, respectively.

As shown in Fig. 6 and Fig. 7, it is seen that when the spacings are equal to 2.0 m and 3.0 m, two blast holes have been completely connected by the cracks regardless of the delay time. In addition, it is also seen that the width of the fracture network along the symmetry axis (red dotted line in Fig. 2) is the narrowest when the delay time is equal to 0.0 ms. As shown in Fig. 8, when the spacing increased to 4.0m, the cracks yielded from two holes can overlap each other near the symmetry axis only when the two holes are blown up simultaneously, whereas the cracks cannot completely connect two blast holes once the millisecond blasting was implemented in the other five cases.

Obviously, the amount of cracks intersecting with the symmetry axis can be considered as an index to evaluate the connectivity and the width of the fracture network between the two blast holes. Figure 9 provides a comprehensive amount of these cracks extracted from the results of Fig. 6 to Fig. 8, to further quantitatively analyze the distribution characteristics of the fracture network induced by rock blasting. In Fig. 9, the horizontal and vertical axis denote the delay time and the amount of cracks, respectively.

On the other side, it is supposed that Δt represents the delay time, L is the spacing between two blast holes, a is the radius of the blast hole, t_{dc} is the duration of the entire pressure-time history in Fig. 4. If $\Delta t > (L\text{-}2a)/C_p + t_{dc}$, it indicates that shock waves from two blast holes will not collide between the holes; in other words, two blast holes are ignited separately. Otherwise, the shock waves will superpose each other between two adjacent holes. Here C_p is the P-wave velocity in the rock, which is expressed as:

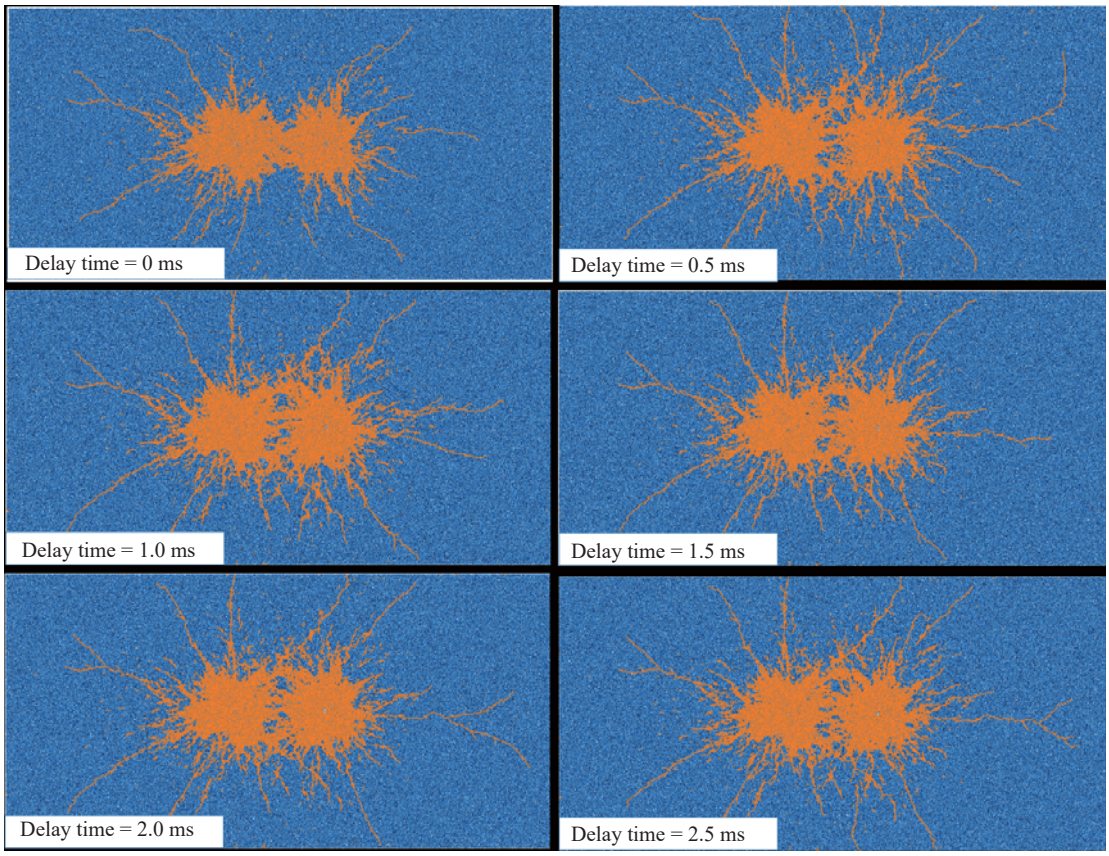

Fig. 6 Distributions of cracks at different delay times (Spacing of two blast holes = 2.0 m)

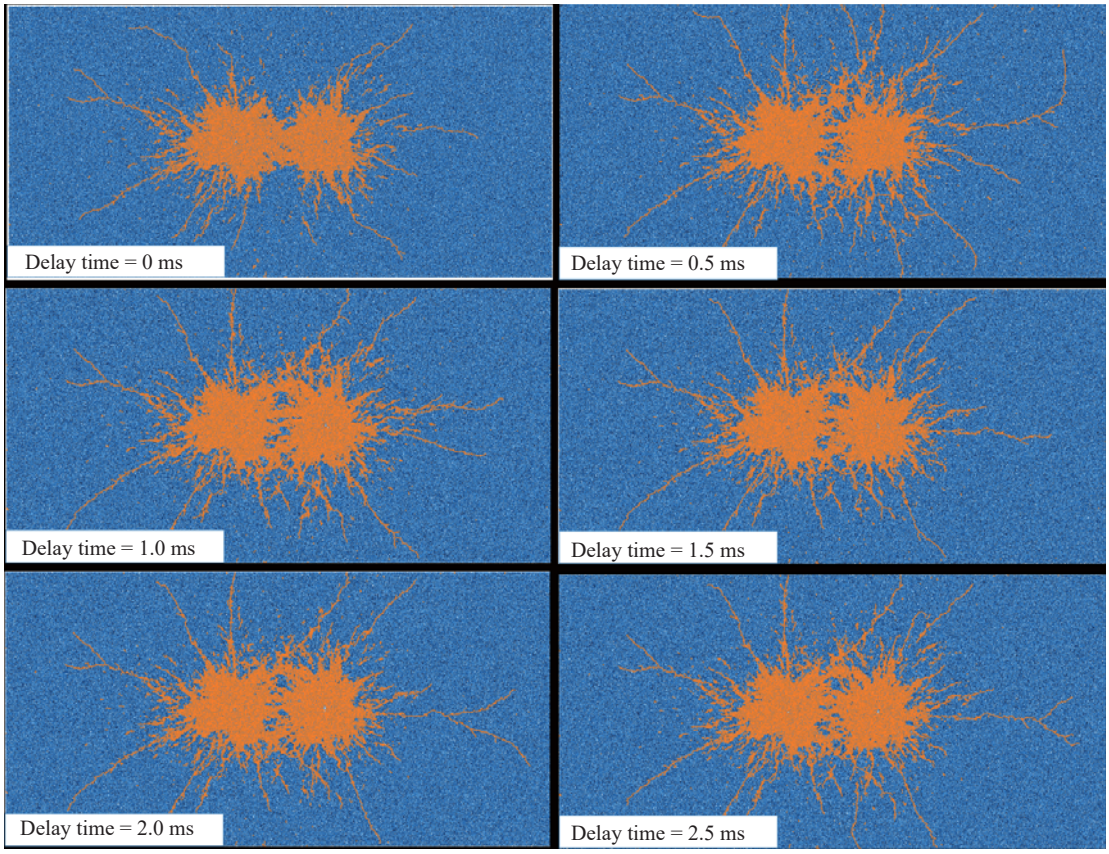

Fig. 7 Distributions of cracks at different delay times (Spacing of two blast holes = 3.0 m)

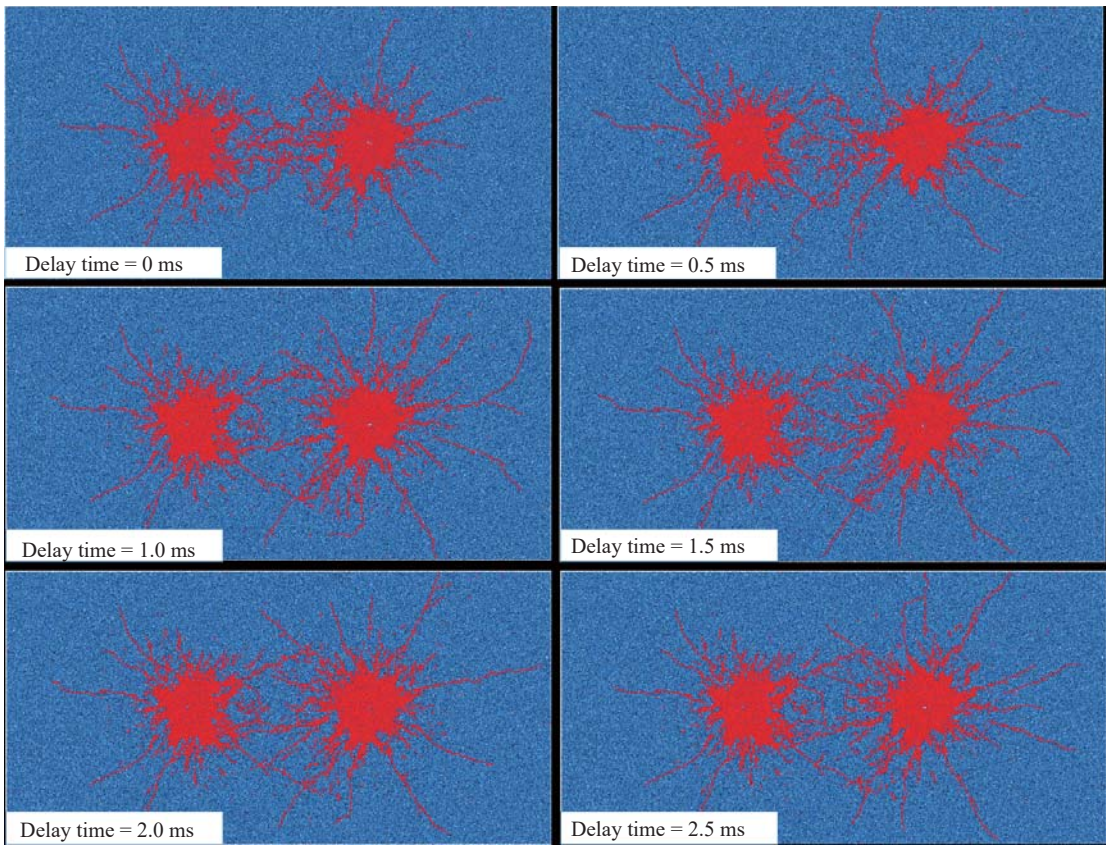

Fig. 8 Distributions of cracks at different delay times (Spacing of two blast holes = 4.0 m)

$$C_{\mathrm{p}}=\sqrt{\frac{\lambda+2\mu}{\rho_0}} \tag{7}$$

where λ and μ are Lamé constants:

$$\begin{cases}\lambda=\dfrac{E\cdot\upsilon}{(1-2\upsilon)\cdot(1+\upsilon)}\\ \mu=\dfrac{E}{2(1+\upsilon)}\end{cases} \tag{8}$$

The relevant material parameters of rock mentioned in Section 2.1 are substituted into Eq. (7) and Eq. (8), and the P-wave velocity in this study can calculated to be 4538 m/s. Thus, the delay times associated with the separate ignition for the cases of different spacing are marked out in Fig. 9.

As shown in Fig. 9, the amount of cracks decreases distinctly along as the spacing between two blast holes increases. When the spacing is equal to 2.0 m and 3.0 m, the amount of cracks increase first and then decrease as the delay time increases. Finally, they stay the same once there are no collisions of shock waves between the two holes. The amount of cracks is minimum under the condition of simultaneous initiation, while it reaches the maximum when the delay time is equal to 0.5 ms. When the spacing is equal to 4.0 m, the amount of cracks decreases monotonically along with the increase of the delay time.

Thus, according to the above discussion, it can be seen that the spacing between two blast holes and the delay time are both critical factors that influence the connectivity and width of the fracture network. Furthermore, the spacing has a more important role than delay time in generating cracks.

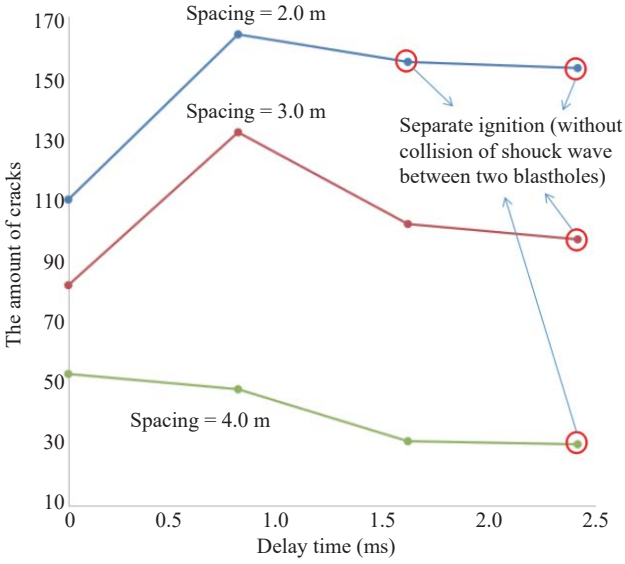

Fig. 9 Amounts of cracks intersecting with symmetry axis in each case

3.2 Compressive stress superposition

In order to explain the phenomenon described in Section 3.1, an analysis from the perspective of stress superposition is carried out. Figure 10 shows the arrangements of monitoring points with the same spacing between any two adjacent points. The spacing is equal to 0.5 m.

Based on the monitoring points arranged as shown in Fig. 10, all the stress histories induced by the dual-blast hole shots can be acquired. The monitoring point located at midpoint of the symmetry axis is selected as a typical case to illustrate the stress superposition between the two blast holes. Figure 11 shows the principal stress histories of this monitoring point for blast hole spacing that is equal to 3.0 m.

As shown in Fig. 11, the first crest of minimum principal stress arrives at the midpoint at 0.38ms; thus, the velocity of the stress wave can be calculated as (1.5 m - 0.06 m) / (0.38 ms - 0.05 ms) = 4500 m/s, which is very close to the theoretical value based on Eq. (7). In addition, the compressive superposition stress for the case of $\Delta t = 0$ ms has nearly twice the amplitude of the single blast hole plus. When two blast holes are ignited with a delay time, two crests of minimum principal stress pluses can be distinctly distinguished, and the stress crest induced by the first ignited blast hole is higher than that induced by the second ignited blast hole. The difference between these two stress crests decreases as the delay time increases. Obviously, there is intense compressive stress superposition between the two blast holes. When two blast holes are ignited simultaneously, the crests of the stress plus from the two blast holes arrive at the midpoint at the same time, inducing the stress superposition at the same direction. Once the Δt is greater than 0.0 ms, the stress plus from the first blast hole may partially offset the compressive stress from the second blast hole, so that the second crest of the stress history at midpoint is obviously less than the first crest. As the delay time increases, the stress pluses from the two blast holes may not meet between the two blast holes, which is similar to when two single stress pluses pass through the midpoint.

Figure 12 shows the peak values of the minimum principal stress histories of all the monitoring points for different delay times and blast hole spacings, and its horizontal axis represents the corresponding number of

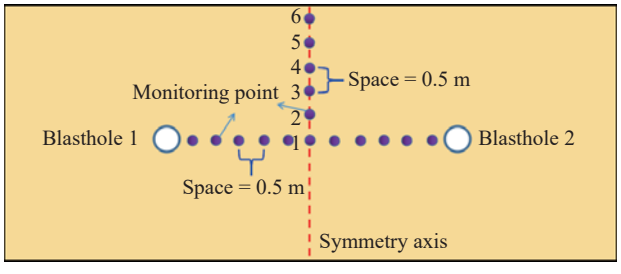

Fig. 10 Arrangements of monitoring points between two adjacent blast holes

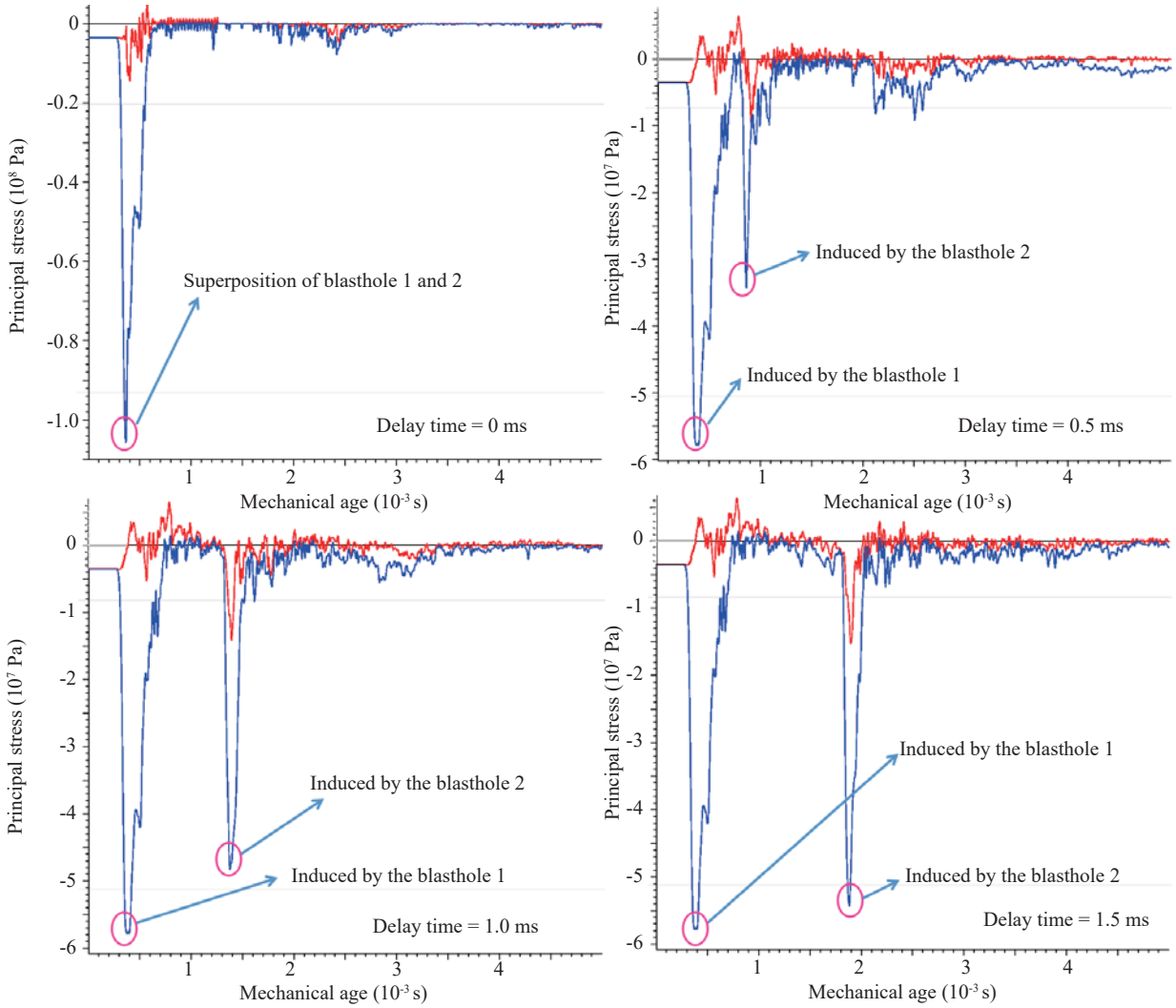

Fig. 11 Principal stress histories of midpoint for the case of blast hole spacing being equal to 3.0 m (Blue lines and red lines represent minimum and maximum principal stresses, respectively. Tensile stress is positive and compressive stress is negative.)

all the monitoring points. No matter how the delay time changes, the peak values of the minimum principal stress histories are all the same if the spacing of the blast hole remains unchanged. Thus, the curves for the peak values of the compressive stress histories are only classified into simultaneous initiation and millisecond ignition at each blast hole spacing, as shown in Fig. 12. Obviously, they have the same variation characteristics along the symmetry axis even if the spacing of the blast holes are different: (a) the maximum compressive stresses at each monitoring point induced by simultaneous initiation are all greater than those induced by millisecond ignition; and (b) the peak value of the compressive stress history located at monitoring point 2 (deviating from spacing direction 0.5 m) is maximum compared with all the other monitoring points. If compressive stress is thought to be

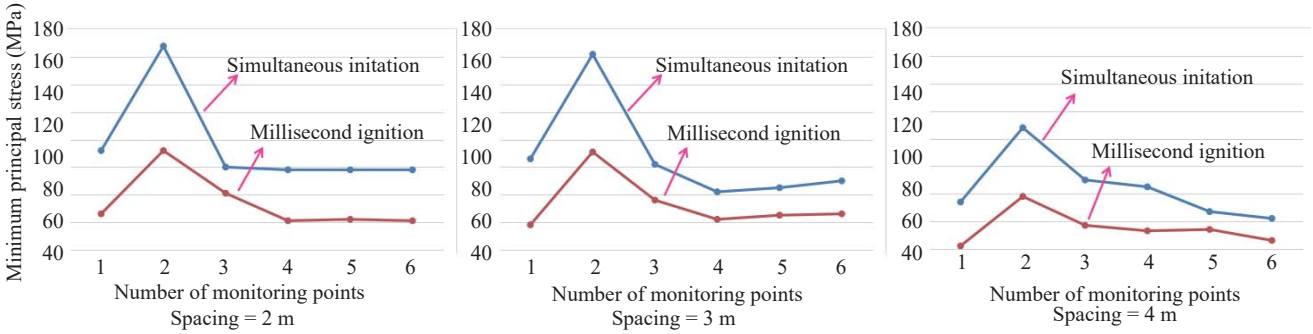

Fig. 12 Peak values of minimum principal stress histories of all the monitoring points (compressive stress)

the dominant triggering factor for the distribution of cracks, according to the peak values in Fig. 12, it can be concluded that the amount of cracks intersecting with the symmetry axis would be maximum for the case of simultaneous initiation, and this amount would remain unchanged regardless of the different delay times. However, these conclusions are obviously in conflict with the results shown in Fig. 8 and Fig. 9. Thus, it can be concluded that the compressive stresses have no apparent influence on the distribution of cracks.

3.3 Tensile stress interactions

Figure 13 shows the maximum tensile stresses of all the monitoring points for the different delay times and blast hole spacings, and the horizontal axis represents the corresponding number of monitoring points. As shown in Fig. 13, the maximum tensile stress located at monitoring point 2 (deviating from spacing direction 0.5 m) is greater than all the other monitoring points for each case, and the locations for the minimum tensile stress in Fig.13 are all that the distances deviating from the spacing direction approximate to be half of blast holes spacing. In addition, when the blast hole spacings are equal to 2.0 m and 3.0 m, the tensile stress of all the monitoring points with 0.5 ms delay time are roughly greater than the other initiation modes; when this spacing increases to 4.0 m, simultaneous ignition could yield maximum tensile stresses at all the monitoring points. Compared with the results in Fig. 9, the amounts of cracks reach the maximum value with 0.5 ms delay time when the blast hole spacing is equal to 2.0 m and 3.0 m, and the amount of cracks is maximum with 0.0 ms delay time when the blast hole spacing is equal to 4.0 m. These conclusions coincide with the characteristics of tensile stress shown in Fig. 13.

In order to further illustrate the effect of delay time on crack amounts, it is necessary to investigate the evolution law of maximum tensile stress as it changes along with the delay time. Figure 14 shows the curves of all the monitoring points for the different blast hole spacings. When blast hole spacings are equal to 2.0 m and 3.0 m, the maximum tensile stresses of most monitoring points increase first and then decrease along as the delay time increases. Nevertheless, when blast hole spacing is equal to 4.0 m, the maximum tensile stresses decrease monotonously as the delay time rises. These change rules are exactly the same as the changes of crack amounts along with the delay time, as shown in Fig. 9. Thus, this indicates that tensile stress plays an important role in manufacturing cracks, and the delay time can indirectly affect the crack amounts by directly influencing the tensile stress.

Unfortunately, as shown in Fig. 14, the maximum tensile stresses when the blast hole spacing is equal to 2.0 m are not greater than when it is induced under the conditions of the other two blast hole spacings. This indicates that the amount of cracks is not the maximum among these three blast hole spacings, which does not conform to the results shown in Fig. 9. Thus, the effect of tensile stress on crack distribution may be a complex question, and it is necessary to further investigate this problem by taking other possible influence factors into account.

3.4 Particle vibration

As mentioned in Section 2.1, rock stratum is made up of a serial of particles, and any two adjacent particles are linked by a parallel-bond model. In fact, a particle

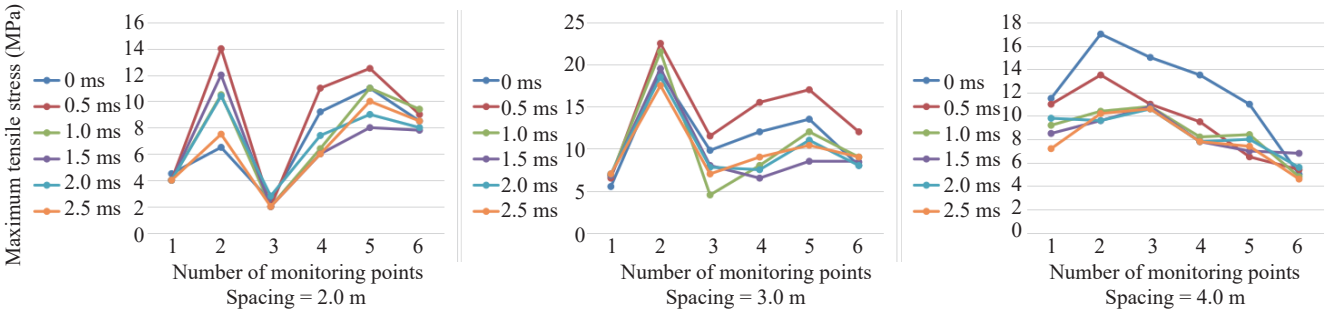

Fig. 13 Peak values of maximum principal stress histories of all the monitoring points (tensile stress)

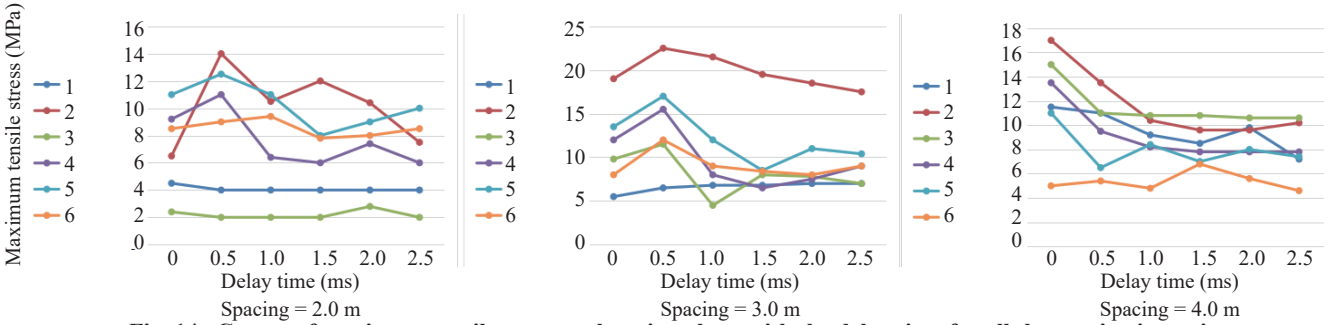

Fig. 14 Curves of maximum tensile stresses changing along with the delay time for all the monitoring points

may have contact with one or more other particles, and multi-bonds may surround this particle. Once one or more bonds are ruptured by the tensile stress, the constraints from other particles are sure to weaken. Furthermore, if all the bonds are invalid, this particle could be an isolated and free granule. Under the action of the shock wave originating from the blast hole, this particle would perform a drastic oscillation and fiercely strike adjacent particles. This phenomenon could bring additional actions to promote the growth of cracks. Thus, the particle vibration histories may provide another approach to understand the influence of blast hole spacing on the distribution of cracks. Figure 15 shows the histories of the unbalanced force of a particle located at monitoring point 2 to illustrate its vibration accelerated velocity.

As shown in Fig. 15, regardless of how the delay time changes, the histories of unbalanced force of the monitoring point manifest an identical variation law; that is, the amplitudes of history curves monotonously decrease as the blast hole spacing increases. In fact, due to the collision and squeezing between adjacent particles, the energy of the shock wave is consumed, so it leads to the sharp decrease of shock wave energy along with an increase in the distance of the radial direction of the blast hole. Thus, it indicates that the increased blast hole spacing induces the shock actions from isolated particles or particles with reduced constraints would decrease around the symmetry axis of the entire model. Compared with the results shown in Fig. 9 for all the

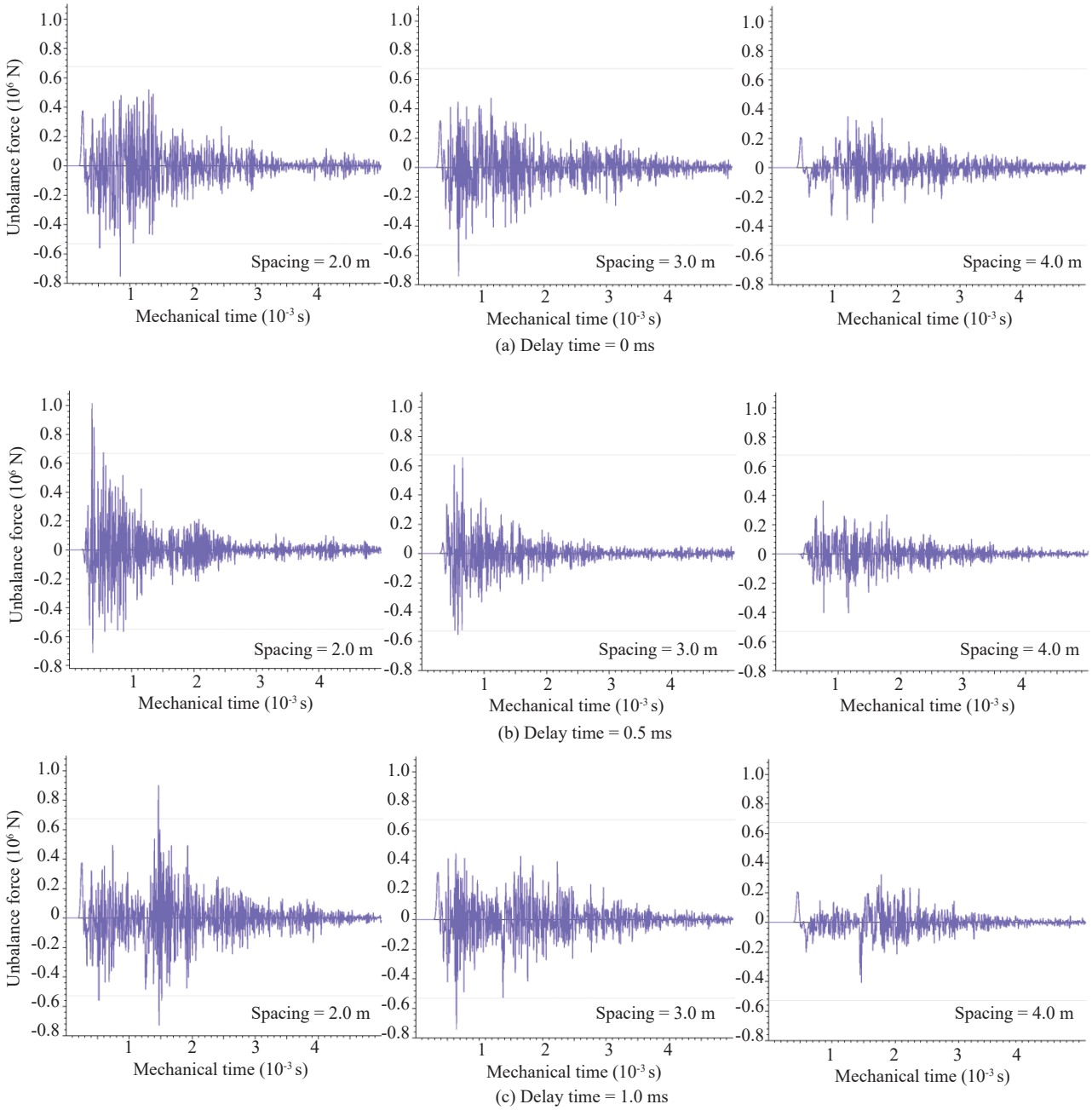

Fig. 15 Histories of unbalance force for the cases of different delay times and blast hole spacings (monitoring point 2)

different delay time cases, as the distance between two holes becomes smaller, more cracks are generated near the symmetry axis. It is concluded that particle vibration plays a more important role than tensile stress in yielding of the cracks, and the blast hole spacing could significantly affect the amount of cracks by influencing the particle vibration around the symmetry axis.

4 Conclusions

Based on the discrete element method, a series of numerical tests considering different blast hole spacings and delay times of millisecond blasting are executed to study their effect on generating cracks. The main conclusions are as follows:

(1) Compressive stress superposition has little effect on crack distribution; however, tensile stress interaction and particle vibration have a significant influence on the connection of cracks between two blast holes. According to the histories of the maximum tensile stresses and unbalance forces of the monitoring points for different delay times, it is concluded that tensile stress interactions are mainly affected by the delay times of millisecond blasting, and particle vibrations around the symmetry axis are primarily affected by the blast hole spacings.

(2) Blast hole spacing plays a more important role than delay time in improving the connectivity and width of the fracture network. The delay time can also have an influence on manufacturing cracks in rock blasting; however, whether it works depends on the distance between the two holes. Once the spacing is beyond a certain range, a longer delay time could weaken the interaction of the shock wave, leading to a decrease of the crack amount.

Acknowledgement

The authors gratefully acknowledge the support of the National Science Foundation for Young Scientists of China (No. 51709176), National Natural Science Foundation of China (No. 51979170), Hebei Province Natural Science Foundation for Yong Scientists (No. E2018210046), Open Project of State Key Laboratory of Advanced Electromagnetic Engineering and Technology (No. AEET 2019KF005) and Key Project of Hebei Natural Science Foundation (No. F2019210243).

References

Chiappetta F (2010), "Combining Electronic Detonators with Stem Charges and Air Decks," http://www.iqpc.com/redForms.aspx?id=414254&sform_id=473344. Accessed 10 Aug., 2012.

Cho SH and Kaneko K (2004). "Rock Fragmentation Control in Blasting," *Materials Transactions*, **45**(5): 1722–1730.

Dohyun P, Byungkyu J and Seokwon (2009), "A Numerical Study on the Screening of Blast-Induced Waves for Reducing Ground Vibration," *Rock Mechanics and Rock Engineering*, **42**: 449–473.

Fakhimi A and Villegas T (2007), "Application of Dimensional Analysis in Calibration of a Discrete Element Model for Rock Deformation and Fracture," *Rock Mechanics and Rock Engineering*, **40**: 193–211.

Henrych J (1979), *The Dynamics of Explosion and Its Use*, New York: Elesvier Scientific Publishing Company.

Itasca Consulting Group Inc. (2015), "PFC2D-Particle Flow Code in Two Dimensions," *Ver. 5.0, User's Manual. ICG, Minneapolis.*

Johansson D and Ouchterlony F (2013), "Shock Wave Interactions in Rock Blasting: the Use of Short Delays to Improve Fragmentation in Model-Scale," *Rock Mechanics and Rock Engineering*, **46**: 1–18.

Park BK, Lee IM, Kim SG, Lee SD and Cho KH (2004), "Probabilistic Estimation of Fully Coupled Blasting Pressure Transmitted to Rock Mass. II: Estimation of Rise Time," *Tunnelling and Underground Space Technology*, **6**(1):25–39.

Rossmanith HP (2002), "The Use of Lagrange Diagrams in Precise Initiation Blasting, Part I: Two Interacting Blast Holes," *Fragblast: International Journal for Blasting and Fragmentation*, **6**(1): 104–136.

Rossmanith HP and Kouzniak N (2004), "Supersonic Detonation in Rock Mass: Part 2—Particle Displacements and Velocity Fields for Single and Multiple Non-Delayed and Delayed Detonating Blast Holes," *Fragblast: International Journal for Blasting and Fragmentation*, **8**(2): 95–117.

Sjöberg J, Schill M, Hilding D, Yi C, Nyberg U and Johansson D (2012), "Computer Simulations of Blasting with Precise Initiation," In: *Rock Engineering and Technology for Sustainable Underground Construction Proceedings, Eurock 2012 - ISRM international symposium*, Stockholm, 28–30 May, 2012.

Vanbrabant F and Espinosa A (2006). "Impact of Short Delays Sequence on Fragmentation by Means of Electronic Detonators: Theoretical Concepts and Field Validation," In: Fragblast 8, *Proceedings of the 8th international symposium on rock fragmentation by blasting, Editec SA*, Santiago, 326–331.

Wang T, Zhou W, Chen J, Xiao X, Li Y and Zhao X (2014), "Simulation of Hydraulic Fracturing Using Particle Flow Method and Application in a Coal Mine," *International Journal of Coal Geology*, **121**: 1–13.

Wang Wei, Li Xiaochun, Yuan Wei, Wang Qizhi and Li Guifeng (2016), "Model Test and Mechanism Study of the Blasting-Enhanced Permeability of Sandstone-Type Uranium Deposits of Low-Permeability," *Chinese Journal of Rock Mechanics and Engineering*, **35**(8): 1609–1617.

Yan Peng, Lu Wenbo, Zhang Jing, Zou Yujun and

Chen Ming (2017), "Evaluation of Human Response to Blasting Vibration from Excavation of a Large Scale Rock Slope: A Case Study," *Earthquake Engineering and Engineering Vibration*, **16**(2): 435–446.

Yi Changping, Daniel Johansson, Ulf Nyberg and Ali Beyglou (2016), "Stress Save Interaction Between Two Adjacent Blast Holes," *Rock Mechanics and Rock Engineering*, **49**: 1803–1812.

Zhu WC, Gai D, Wei CH and Li SG (2016), "High-Pressure Air Blasting Experiments on Concrete and Implications for Enhanced Coal Gas Drainage," *Journal of Natural Gas Science and Engineering*, **36**: 1253–1263.

Zhu WC, Wei CH, Li S, Wei J and Zhang MS (2013), "Numerical Modeling on Destress Blasting in Coal Seam for Enhancing Gas Drainage," *International Journal of Rock Mechanics & Mining Sciences*, **59**: 179–190.